Flood Inundation Mapping of Dikhow River Basin of Assam

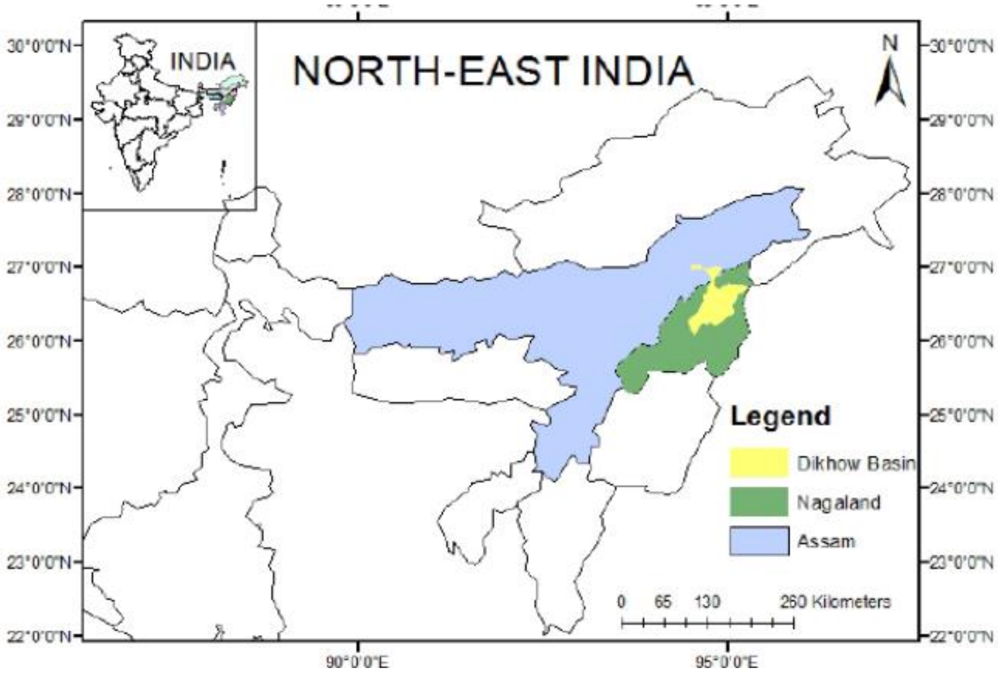

आपो हिष्ठा मयो भुवः

NATIONAL INSTITUTE OF HYDROLOGY
Centre for Flood Management Studies
Dispur, Guwahati - 781 006
2024-25

ABSTRACT

Flood is one of the most destructive events. Accurate and current floodplain maps are most valuable tools for avoiding severe social and economic losses.Early identification of flood-prone properties during emergencies allows public safety organizations to establish warning and evacuation priorities. This study has been undertaken for the Beki river basin based on the recommendation by the Chief Engineer, WRD Assam.

Dikhow River is one of the largest tributaries of the Brahmaputra river basin originating from Yezami village near Zunheboto town of Nagaland. It debouches into the mighty river Brahmaputra River at Dikhowmukh, Sivasagar district, Asam covering a length of 255.8 km contributing 0.7% runoff. The geographical area of the Dikhow catchment is approximately 3100 km^2, covering 85% of Nagaland, 10% of Assam and 5% of Arunachal Pradesh.

One of the objectives of the study is to assess usefulness and limitations of RRI model for flood inundation modelling for an Indian basin. The other major objective is to prepare flood Inundation maps for Dikhow river basin. In this study, the RRI model is proposed to be used to model the flood inundation area by simulating rainfall runoff process and river routing.

The study group consists of Dr. Sanjay Kumar Sharma, Scientist-‘D’, Swapnali Barman Scientist ‘D’ , W. R. Singh, Scientist ‘C’ and Siddharth Arora , Scientist ‘, under the work programme for 2024-25.

CONTENTS

LIST OF FIGURES

1.0 INTRODUCTION

Flood is a temporary effect of inundation of water partially or completely over the areas adjoining Rivers, Lakes and other water bodies due to overflow due to rapid accumulation of runoff. Flood is worst natural as well as anthropogenic induced disaster which causes havoc affecting social life and economy millions of people every year. Flood accounts 40% to that of the disasters and 50% deaths among the disasters caused every year. The data shows that flood is undoubtedly the worst destructive phenomenon in the world and is a consequence of increasing frequency of extreme precipitation events (Salunkhe et al. 2018).

Flood damage has been extremely severe in recent decades due to increase in the frequency and intensity of floods. India, due to its geographical location, climate, topography and large population, witnesses greater impact of flood disasters. Floods have been a recurrent phenomenon in India and cause huge losses to lives, properties, livelihood systems, infrastructure and public utilities (NDMA 2008).According to National Disaster Management Authority, out of a total geographical area of 329 million hectares in India, about 40 million hectares is prone to floods. Flood affects 75lakh hectares of land on an average every year (NDMA2008). On an average, loss to life is about 1590 and a loss in financial term is 13,000 million rupees due to flood (Gopalakrishnan 2002).

Flooding of the plains and valleys during wet season is a common hazard in north east India. Most of the flooding occurs in Brahmaputra river basin. The geographic spread of Brahmaputra river basin contains extensive flood plains and fresh alluvium deposits. During the monsoon season, i.e., June–September, floods seem to be a common occurrence in the geographical area of Brahmaputra River. Heavy rainfall in the hill segment as well as in the plains, lack of adequate gradient to drain out the high discharge of the rivers, increasing silt load due to high rates of deforestation and landslide in the upper catchment and breaching of embankments are the main causes of flood in this region (Gogoi et al.2013).

Flooding in the North East India region is affecting large number of population particularly in Assam every year. So flood hazard monitoring and mapping is need of the hour. While monitoring flood hazards and processes that lead to form the bases for early warning systems, flood hazards zoning often provide the major prerequisite components for flood disaster management. Decision makers need to know the magnitude of flooding. Flood hazard zones can be delineated using remote sensing, geographical information system (GIS), and hydro-dynamic modelling tools with the help of data from flood stage/river gauge water levels. In the recent years, the integration of information extracted through remote sensing and GIS with other datasets provides tremendous potential for identification, monitoring and assessment of flood disaster (Pradhan et al. 2009; Duttaet al. 2010).

Flood management needs the utilization of hydrological and hydraulic records of data at various spatial and temporal resolutions. It can be accomplished with model simulations and calibrations with measured data at certain locations and selected time intervals. To better understand the impact of river gauge levels in the surrounding floodplain, there is a need for translating this water level/discharge information into spatial domain and visualizing the effects of flood in the floodplain. One dimensional (1D) and two dimensional (2D) hydrodynamic models can be used for this purpose. The benefits of these models are their ability to show the direction and magnitude of flow on riverbed and floodplains. Ideally, the numerical model for simulating hydrodynamic behavior of the river and floodplains should possess the qualities of handling complex topography, ability to simulate the sub-critical and supercritical flow, steady and unsteady flow, continuous and discontinuous flow in case of dyke breaching or dam breaking problems, ability to simulate flows through the hydraulic structures. This model provides hazard parameters like waterlevel, depth of inundation and flow velocities at every grid point.

This study is carried out with the help of 1D, 2D hydrodynamic model using HEC RAS in Beki River Basin. Data used are, ASTER DEM (Advanced Spaceborne Thermal Emission and Reflection Radiometer), SRTMDEM (Shuttle Radar Topographic Mission) of 30 m & 90 m resolution. Landsat 5, 7 & 8 data of 15 m, 30 m and Sentinel 2 data of 10 m, 20 m are the Satellite Data used for visualization in the Study. Discharge monitoring Station of Assam State Water Resources Department & CWC is available in the downstream of the Beki River Basin.

1.1 1D, 2D Hydrodynamic Modelling

Flood inundation mapping is an important tool for State and district level planning, emergency action plans, flood insurance and ecological aspects. Mapping a floodplain requires a forecasting/observation of the behavior of the stream for various recurrence interval storm events and the ability to translate the forecasted results into a plan-view extent of flooding. The Hydrologic Engineering Center's River Analysis System (HEC-RAS) has the ability to model flood events and produce water surface profiles over the length of the modeled stream. With the companion GIS utility, HEC-GeoRAS, those water surface profiles can easily be converted to flood inundation maps. This study will address the steps required to perform a flood inundation mapping study using HEC-RAS and will present a work conducted for Beki river one of the tributaries of Brahmaputra river, demonstrating the capabilities of HEC-RAS and HEC-GeoRAS (Goodell et al. 2006).

Standard flood modelling practices include 1D modeling (upstream to downstream direction), 2D modeling (downstream and lateral directions), hybrid 1D–2D modeling and 3D numerical models, along with hydrograph design, specified ground roughness, and accurate digital elevation data. 2D modelling uses multi-scenarios in order to define the areas with risk of flooding in a complex urban environment; where it cannot be assumed that all flow will be parallel to the main river and where a higher hydrodynamic accuracy is required. The 2D HEC-RAS multi-scenario provides a more realistic perspective about the floods and possible flood threats and has shown to be a valuable asset in the improvement process in case of Modelling flood inundation area with the help of High resolution and precise terrain models. 2D Hydraulic Modelling in relation to watercourses describes water movement through space in three directions. 2D Hydraulic Modelling along the river channel uses lateral direction (e.g., whenever the water begins to spill out overland) and vertical direction which practically defines the height of the flood. Two-dimensional flood propagation modeling offers additional information regarding some characteristics of the flood such as vertical and horizontal flow velocity as well as water trend propagation.

HEC-RAS version 5.0 integrated 2D unsteady flow capabilities, offering the possibility to analyse water propagation over a predefined surface, which is found in the form of a digital elevations model. HEC-RAS is a well-known software, capable of modeling a flood inundation event. The scenarios proposed by this study are to be simulated using the open source HEC-RAS software 5.0.5 version, developed by U.S. Army Corps of Engineers (USAGE). Starting with HEC-RAS software version 5.0, two-dimensional unsteady water flow modeling can be performed. The program 2D flow modeling algorithm solves shallow water equations, also called bi-dimensional Saint Venant equations / 2D diffusion wave equations (Mihu-Pintilie et al. 2019).The ability of an un-calibrated 2D flood routing model to produce reliable flood simulations mostly depends on the quality of inputted topography and surface roughness data and the level at which these data are captured in computational mesh structure. These two key inputs to which 2D models exhibit high sensitivity are generally given in the form of digital surface model (DSM) and land cover raster, respectively. The availability of several DSM and land cover products from a variety of sources at a wide range of resolutions and significantly increasing acquisition cost as resolution increases makes it difficult to select the optimal scales of input data that can stabilize model predictions. Hence, it is important to examine the impacts of varying the level of detail of input data on the responses of 2D hydrodynamic models. These examinations should be model based due to possible differences in data processing techniques applied by 2D models in assigning elevation and surface roughness values to computational mesh elements (Yalchin. 2020)

1.2 Remote Sensing & GIS in Flood Modelling Applications

Remote sensing can provide information on flood inundated areas for different magnitudes of floods so that the extent of flooding can be related to flood magnitude. The duration of flooding can be estimated in view of multiple coverage of the same area within 2-3 days by using multi satellites. High resolution satellites data provide information on the flood plain and details of flood control works. Specific flood return periods can be estimated using the extent of inundation mapped using satellite data. Contour information is used in the inundation extent for a given water level elevation can be estimated, which is used as a vital input for risk zone mapping.

In the last two decades, research in remote sensing has significantly contributed to the availability of a variety of hydro-meteorological data, which are providing new opportunities to modelling ungauged basins. Most of such data products are freely available to everyone. The synergistic advances in software, particularly geographic information systems, are making it possible to effectively process the available data. This motivates exploring the possibilities of hydrological and hydraulic simulations for diverse catchments, which hitherto remained impossible. Remote Sensing data were used as input to distributed hydrological models to better predict streamflow. Recent advanced applications showed the ways of combining the output of distributed hydrological models with hydraulic models and of assessing flood extents in medium to large scale catchments (Bhattacharya et al. 2019).

Satellite remote sensing coupled with Geographical Information System (GIS) has a powerful role in monitoring and mapping flood inundated and drainage congested areas.

Remote sensing data acquired in the visible, near infrared (IR) and short-wave infrared (SWIR) regions have shown encouraging results in providing information on spatial pattern of flood inundation. Both pre- and post-monsoon period data are required for delineation of flood inundation and flood affected areas. The flood inundation mapping through computer-assisted digital analysis approach is based solely on their spectral response pattern as seen in the image or as portrayed in the changes in spectral radiance or brightness temperature values of space-borne multi-spectral data. This, in turn, is a cumulative effect of terrain's relief, vegetation cover, wetness, etc.

In False Colour Composite (FCC), water is represented by dark blue or black colour. Colour of shallow water slightly changes from dark blue to light blue. Flooding is confined in the low-lying areas, local depressions and lower element of the slope. Such areas have either standing water or a thin film of water or surface wetness during flood season while they remain almost dry during pre-monsoon seasons. The base data showing the administrative boundaries, population details, agricultural activities, important places, communication networks and other infrastructure details may be prepared well in advance of the monsoon season. The availability of satellite data may be prepared well in advance.

Various satellites having sensors which operate both in optical as well as in microwave region of Electro Magnetic Spectrum at different spatial resolutions can be used for obtaining information regarding the availability of satellite data. The reference map of all the individual satellites are readily available and are used for identifying the path and row numbers of the satellite coverage in the area of interest. Based on the orbital calendar of the satellite, the date of pass of satellite can be known in advance. Advantages of the information acquired by satellite remote sensing are of synoptic coverage, repetivity and especially in the easiness to compare the data before, during and after floods. Inundation extent for specific flood return periods can also be estimated. The increasing availability of very high performance GIS software packages such as Arc-GIS and ARC/INFO offers new opportunities for engineers to perform flood inundation analysis with interactive visualization within immersive decision support environments. The GIS technology has the ability to capture, store, manipulate, analyze, and visualize the diverse sets of geo-referenced data.

2.0 REVIEW OF LITERATURE

Flood is a serious problem in Assam as the entire state is dependent on the Brahmaputra valley bestowed with wide floodplains. It is also surrounded by Eastern Himalayas in the North, Karbi Anglong and Naga Hills in the East, Jaintia and Kasi hills in the South as well as Garo Hills in the west. These hills are responsible for number of localized intensive precipitation events causing distributed floods at various scales and intervals (Arun G. et al. 2020).Flood Inundation Mapping is an important tool for engineers, planners, and government agencies used for municipal and urban growth planning, emergency action plans, flood insurance rates and ecological studies. By understanding the extent of flooding and floodwater inundation, decision makers are able to make choices about how to best allocate resources to prepare for emergencies and to generally improve the quality of life.

The Hydrologic Engineering Center’s River Analysis System (HEC-RAS) is a software package that is well-suited for developing flood inundation maps for a variety of applications. An HEC-RAS model can be used for both steady and unsteady flow, and sub- and supercritical flow regimes. With its companion utility, HEC-GeoRAS and ArcView, seamless integration with GIS makes both the construction of the model geometry and the post-processing of the output very easy (Goodell et al. 2006). Manas/Beki is one of the Himalayan Trans boundary rivers flows through China, Bhutan and India. It is one of the North bank tributary of the River Brahmaputra. Flood and Sediment Transport are the Major issues in the River Basin. The Manas River receives the snowmelt in summer, even though the major flood discharges originate from the rainfall in the beginning of the southwest monsoon with peak discharge during July to September (Singh V. P. et al. 2004).

The River passes through large area of alluvial plains of Barpeta, Assam before Confluence at River Brahmaputra. To the east and west of the Barpeta area, a group of lakes occupy shallow depressions which may possibly indicate the inter-wedged back swamps of the Manas-Beki River system and also of the main Brahmaputra River. The local precipitation and small perennial channels help sustain these lakes all through the year. Some lakes are cut-off oxbows of the older channels and are sustained by groundwater flow as well as by the small rivers/streams emerging from the peripheral area. In the inselberg zone, some large lakes occur in 5 to 10 m depressions in the Chapar Formation (Lower part of the basin). Besides the receiving of much surface runoff from the stream of the inselberg zone these lakes also have a direct contact with the water table. Thus both the surface and the subsurface flows have an equilibrium outlet through streams feeding the main Brahmaputra River. During high floods these outlets also act as channels of back flooding. The progressive reduction of these lakes through reclamation and conversion to paddy lands in the proximity of Manas, Beki and Brahmaputra causes marginal transpirational loss of waters which ultimately may upset the long term balance of the runoff systems. The River Beki flows 198 km respectively through the Assam Valley before meeting the Brahmaputra (Singh V. P. et al. 2004).

Efficient water resources management requires the availability of hydrological and hydraulic information at various spatial and temporal scales. Collection of hydro-meteorological data for a large basin is hampered by several reasons such as high operational costs, availability of limited road network, shortages of technical manpower and accessibility issues due to difficult terrains. Additionally, in trans-boundary basins data sharing practices may cause an extra challenge to accessing collected data(Bhattacharya et al. 2019).The hydrological and hydraulic studies with better availability of Hydro-met and Terrain data reasonably well encapsulate the hydrological and hydraulic processes although the uncertainty in model predictions are rather high in data scarce environment (Bhattacharya et al. 2018).

Horitt M. S. et al 2002, tested 1D and 2D models of flood hydraulics (HEC-RAS, LISFLOOD-FP and TELEMAC-2D) for a 60 km reach of the river Severn, UK. Radar Remote Sensing satellite based synoptic views of flood extent have been acquired for flood certain flood events. The three models were calibrated, using floodplain and channel friction as free parameters, against both the observed inundated area and records of downstream discharge. The predictive power of the models calibrated against inundation extent or discharge for the individual flood events and related one over other, showed that both the HEC-RAS and TELEMAC-2D models can be calibrated against discharge or inundated area data and give good predictions of inundated area. But, the LISFLOOD-FP needs to be calibrated against independent inundated area data to produce acceptable results. The different predictive performances of the models stem from their different responses to changes in friction parameterisation.

Zope P. E. et al. 2017 used an integrated approach of Hydrological Engineering Centre-Hydrological Modelling System (HEC-HMS), HEC-GeoHMS and HEC-River analysis system (HEC-RAS) with HEC-GeoRAS has been used. These models are integrated with geographic information system (GIS) and remote sensing data to develop a regional model for the estimation of flood plain extent and flood hazard analysis. They came up with the conclusion that the provision of detention ponds reduces the peak discharge as well as the extent of the flooded area, flood depth and flood hazard considerably. The study also showed the impact of floods on different LULC through the change in LULC estimated for the years 1966 and 2009. LULC impact assessment on flood is one of the important aspect highlighted in the study.

Timbadiya P. V. et al 2011, calibrated HEC RAS model through mannings n value in prediction of Flood in lower Tapi river for the year 1998 and 2003. The calibrated model based on channel roughness used for simulation of 2006 floods shown better performances, the RMSE values for the simulated flood and observations of the peak flood shown very close. The study used different manning's roughness values in the upper and lower reach of the stretch and addressed to use so. On simulation of past floods of year 1998 and 2003 for single value of Manning's roughness coefficient, it became evident that different Manning's roughness coefficients are required for upper and lower reaches. Manning's n value varied from 0.035 to 0.025 through the entire stream.

Patel D. P. et al 2017 used 1D/2D coupled hydrodynamic modelling for the Surat city and identified that the HEC-RAS simulation time depends on 2D flow area computation, levees cell spacing and computation interval. Through the trial and error method, it is identified that the optimum computation setting are: point spacing 50 9 50 m, levees cell spacing 50 9 50 m and computation interval of 15 s. The entire simulation under unsteady flow condition runs in 16 h. The system used for simulation has Intel (R) core (TM) i3-4005U CPU 1.70 GHz, 4 GB RAM, 64-bit OS. Further decrease in grid size will increase the run time up to 3–3.5 days. This study provides strong supportive evidence of the potentiality of new HEC-RAS. It is a prime requirement to reduce the data deficiencies and appropriate DGPS and precise hydraulic and the hydrological survey will reduce the uncertainty for 1D/2D couple hydrodynamic modelling. HEC-RAS 5.0 is identified as potential software for flood inundation modelling. The assessment of the HEC-RAS with respect to this peculiar aspect is an important step for successful and improved development of the hydrodynamic model and thus can provide important assistance in building flood mitigation strategies for any similar cased worldwide.

3.0 STUDY AREA

Dikhow River is one of the largest tributaries of the Brahmaputra river basin originating from Yezami village near Zunheboto town of Nagaland. It debouches into the mighty river Brahmaputra River at Dikhowmukh, Sivasagar district, Asam covering a length of 255.8 km contributing 0.7% runoff. The geographical area of the Dikhow catchment is approximately 3100 km^2, covering 85% of Nagaland, 10% of Assam and 5% of Arunachal Pradesh.

3.1 Location

Dikhow River is one of the largest tributaries of the Brahmaputra river basin originating from Yezami village near Zunheboto town of Nagaland. It debouches into the mighty river Brahmaputra River at Dikhowmukh, Sivasagar district, Assam covering a length of 255.8 km contributing 0.7% runoff. The geographical area of the Dikhow catchment is approximately 3100 km2, covering 85% of Nagaland, 10% of Assam and 5% of Arunachal Pradesh. River Dikhu 's major tributaries are Yangyu and Nanung in the Tuensang and Mokokchung district. The Dikhu River is not only a popular tourist attraction but also an important source of people's livelihood. The Dikhu River is a lifeline for millions of people in Assam and Nagaland.

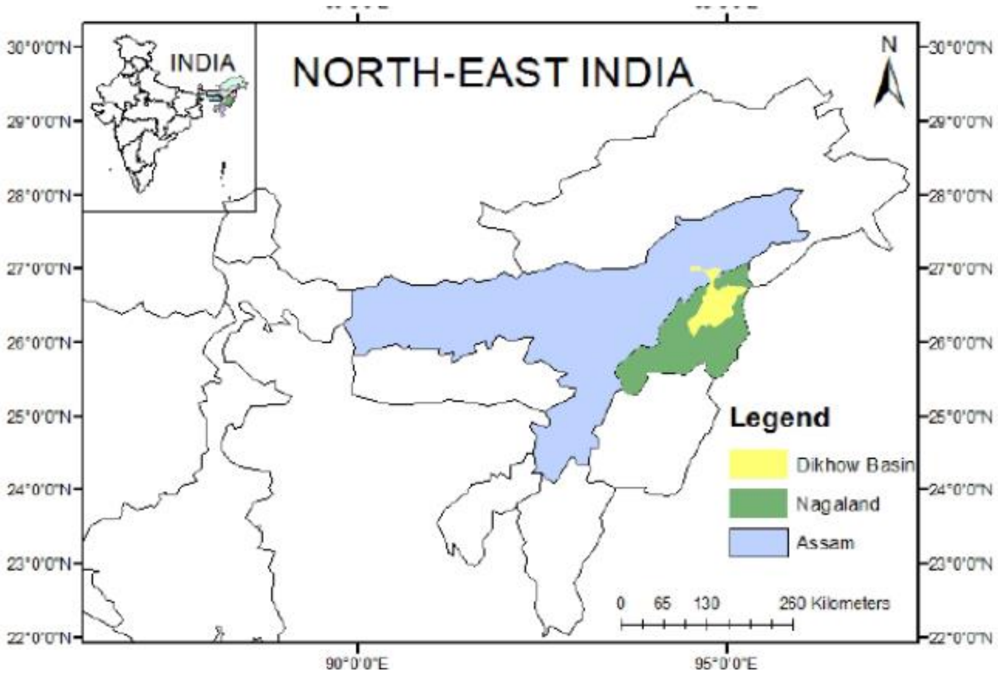

Fig.3.1 Location of Dikhow River Basin

3.3. Climate

The basin experiences four distinct seasons in a year: winter, summer, monsoon and autum/post- monsoon. The winter season begins in December and continues to the end of February. Light north- easterly winds blow down the Brahmaputra valley in Assam and light northerly to north westerly winds in West Bengal. The weather is occasionally changed by the passage of western disturbances across the region, light rainfall occurs in January and February along the hills, increasing towards North-east Assam. The hot weather starts from March onwards and continues up to the last week of May. The monsoon sets in by the last week of May or in early June, being usually ushered in by a depression in the Bay of Bengal. Subsequently, a series of such depressions, forming at the head of the Bay and moving inland, give spells of continuous and moderate to heavy rain generally over the region. July and August are the rainiest months. Almost all the rain in this season is associated with thunder. The monsoon withdraws in the last week of September or the first week of October. After the withdrawal of the monsoon winds, light unsteady winds are experienced by the middle of October. Occasionally, in October, cyclonic storms from the Bay cross the Bengal coast bringing clouds and rain with them. The weather during the autumn remains very comfortable with relatively clear sky and moderate temperature.

3.4. Topography and Basin Characteristics

Dikhow River basin is one of the Trans Himalayan Basin Tributaries of Brahmaputra Basin originates in Tibet where elevation ranges from 7500 m above sea level, runs through the snow cover Himalayan peaks of Bhutan and discharges in the Brahmaputra river basin at Barpeta at an elevation of 28 m above sea level. It has diverse climate zones facing higher amount of precipitation in terms of snowfall as well as rainfall in the North Eastern region of India.

3.5 Temperature

The minimum and maximum temperature of the basin is 16.16°C and 38.79°C respectively during that period. During the winter season in December to January; the minimum temperature over the Basin varies from 16.16°C to 17.56°C. In the rainy season, in the month of July, the mean temperature varies from 32.47°C to 36.17°C. Towards the end of the monsoon season, in the month of October, the temperature over the basin varies from

29.23.0°C to 34.91°C. During the summer season in April and May, the minimum temperature in the Basin varies from 25.67°C to 27.21°C.

The higher elevation zones of the Himalayan ranges (Tibet & Bhutan part) experience lower temperatures than the other regions of the basin. These parts also experiences snowfall as it is a Trans-Himalayan snow fed basin. The southern part of the valley experience hot summer in April and May. During summer, the average maximum temperature in this part of the basin remains above 35°C, whereas the maximum temperature is 40°C. Most of these places above 1,500 m experience ground frost in peak winter month but doesnot experience any snowfall. Altitude range from 2500 - 7500 m above sea level generally experience snowfall during December to March.

3.6 Rainfall

The average annual rainfall is 2371.21 mm. The basin is not affected by drought. The distribution of rainfall in the Brahmaputra basin is different at different parts of the basin. Monsoon rains from June to September account for 60-70 % of the annual rainfall in the basin, while the pre-monsoon season covering the period March through May produces 20-25 % of the annual rainfall caused primarily by depressions moving from the west and by local convectional storms. During the post-winter months, the north-east monsoon finds its way into the Brahmaputra valley through a saddle in the high Himalayas, at their eastern end. The rainfall in the Brahmaputra valley ranges from 2,125 mm to about 4,142 mm.

4.0 METHODOLOGY

The methodology used for the Flood Inundation Modelling for Beki River basin is briefly described in this chapter. The study uses 1D, 2D hydrodynamic routing model which is available in the software platforms such as RRI, Hec-RAS & MIKE Flood. It is commonly used for assessment floods with the help of open channel flow equations using geometries along the river based on observed discharge. There are many applications in water resources fulfilled by creation of 1D, 2D Geometries and application of open channel flow routing. Few main applications are Flood forecasting, Alarming, Flood Inundation Mapping/Modelling, assessment of damage, rescue operations and insurance for affected families.

4.1 RRI MODEL DESCRIPTION

Rainfall-Runoff-Inundation (RRI) model has been used to model the hydrological behavior of the Study Area. RRI is a two-dimensional model capable of simulating rainfall-runoff and flood inundation simultaneously (Sayama, 2012). The model deals with slopes and river channels separately. At a grid cell in which a river channel is located, the model assumes that both slope and river channel are positioned within the same grid cell. The channel is discretized as a single line along its centerline of the overlying slope grid cell. The flow on the slope grid cells is calculated with the 2D diffusive wave model, while the channel flow is calculated with the 1D diffusive wave models. For a better representation of rainfall-runoff-inundation processes, the RRI model also simulates lateral subsurface flow, vertical infiltration flow and surface flow.

The lateral subsurface flow, which is typically more important in mountainous regions, is treated in terms of the discharge-hydraulic gradient relationship, which takes into account both saturated subsurface and surface flows. On the other hand, the vertical infiltration flow is estimated by using the Green-Ampt model. The flow interaction between the river channel and slope is estimated based on different overflowing formulae, depending on water-level and levee-height conditions (Sayama, 2010). The model separates the grid cells as slope and river. The grid cell is assumed as both slope and river within the same grid cell for the location of river channel. RRI couples 1D diffusive wave model for channel flow and 2D diffusive wave model for slope. Figure. 5.1 shows the schematic diagram of RRI model.

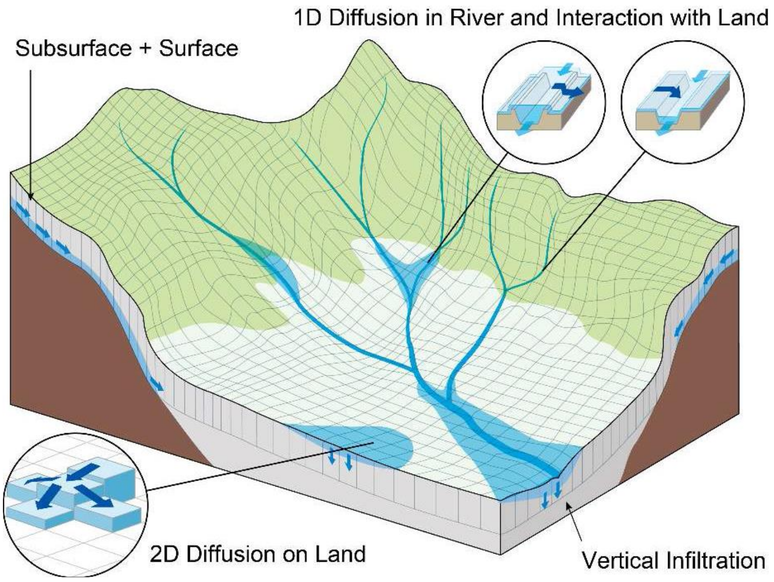

Fig 4.1 Schematic diagram of RRI model

Source: Sayama, 2010

4.2.1 Governing equations of RRI model

A method to calculate lateral flows on slope grid-cells is characterized as "a storage cell-based inundation model" (Hunter, 2007). The model equations are derived based on the following mass balance equation and momentum equation for gradually varied unsteady flow.

$$\frac{\partial h}{\partial t} + \frac{\partial q_x}{\partial x} + \frac{\partial q_y}{\partial y} = r - f \qquad (1)$$

$$\frac{\partial q_x}{\partial t} + \frac{\partial u q_x}{\partial x} + \frac{\partial v q_x}{\partial y} = -gh\frac{\partial H}{\partial x} - \frac{\tau_x}{\rho_w} \qquad (2)$$

$$\frac{\partial q_y}{\partial t} + \frac{\partial u q_y}{\partial x} + \frac{\partial v q_y}{\partial y} = -gh\frac{\partial H}{\partial y} - \frac{\tau_y}{\rho_w} \qquad (3)$$

h = height of the water from the local surface

q_x, q_y = unit width discharges in x and y directions

u, v = flow velocity in x and y directions

r = rainfall intensity

f = infiltration rate

H = height of the water from the datum

ρ_w = density of water

g = gravitational acceleration

τ_x, τ_y = shear stress in x and y directions

The second terms of the right side of (2) and (3) are calculated with the Manning's equation.

$$\frac{\tau_x}{\rho_w} = \frac{g n^2 u \sqrt{u^2+v^2}}{h^{1/3}} \tag{4}$$

$$\frac{\tau_y}{\rho_w} = \frac{g n^2 v \sqrt{u^2+v^2}}{h^{1/3}} \tag{5}$$

where n is the Manning's roughness parameter.

Under the diffusion wave approximation, inertia terms are neglected in left side of equation (2) and (3) and the following equations are derived for x and y direction.

$$q_x = -\frac{1}{n} h^{5/3} \sqrt{\left|\frac{\partial H}{\partial x}\right|} sgn\left(\frac{\partial H}{\partial x}\right) \tag{6}$$

$$q_y = -\frac{1}{n} h^{5/3} \sqrt{\left|\frac{\partial H}{\partial y}\right|} sgn\left(\frac{\partial H}{\partial y}\right) \tag{7}$$

where sgn is the signum function.

The RRI model spatially discretizes mass balance equation (1) as follows:

$$\frac{dh^{i,j}}{dt} + \frac{{q_x}^{i,j-1} - {q_x}^{i,j}}{\Delta x} + \frac{{q_y}^{i,j-1} - {q_y}^{i,j}}{\Delta y} = r^{i,j} - f^{i,j} \tag{8}$$

Where ${q_x}^{i,j}, {q_y}^{i,j}$ are x and y direction discharges from a grid cell at (i,j).

From the equation (6), (7) and (8), water depth and discharge can be calculated for each grid cell for each time step. RRI think about the different discharge hydraulic gradient relationship for surface flow and subsurface flow so it can simulate both condition flows with the same algorithm. RRI model use the following equations, which were originally conceptualized by Ishihara and Takasao (1962) and formulated with a single variable by Takasao and Shiiba (1976,1988) based on kinematic wave approximations.

Equation (9) and (11) describe the saturated subsurface flow and the equation (10) and (12) describe the combination of the saturated subsurface flow and surface flow based on the Darcy law. For the kinematic wave model, hydraulic gradient is assumed to the topographic slope and RRI model assumes the water surface slope as the hydraulic gradient.

$$q_x = -k_a h \frac{\partial H}{\partial x} (h \leq d) \qquad (9)$$

$$q_x = -\frac{1}{n}(h - d_a)^{5/3} \sqrt{\left|\frac{\partial H}{\partial x}\right|} sgn\left(\frac{\partial H}{\partial x}\right) - k_a(h - d_a)\frac{\partial H}{\partial x} (d_a < h) \qquad (10)$$

$$q_y = -k_a h \frac{\partial H}{\partial y} (h \leq d) \qquad (11)$$

$$q_y = -\frac{1}{n}(h - d_a)^{5/3} \sqrt{\left|\frac{\partial H}{\partial y}\right|} sgn\left(\frac{\partial H}{\partial y}\right) - k_a(h - d_a)\frac{\partial H}{\partial y} (d_a < h) \qquad (12)$$

where k_a is the lateral saturated hydraulic conductivity and d_a is the soil depth times the effective porosity.

The following equations (13) and (14) can be also used to simulate the effect of unsaturated, saturated subsurface flow and surface flow with the single variable of h (Tachikawa, 2004) (Sayama M. , 2009).

$$q_x = \begin{cases} -k_m d_m \left(\frac{h}{d_m}\right)^{\beta} \frac{\partial H}{\partial x}, & (h \leq d_m) \\ -k_a(h - d_m)\frac{\partial H}{\partial x} - k_m d_m \frac{\partial H}{\partial x}, & (d_m < h \leq d_a) \\ -\frac{1}{n}(h - d_a)^{5/3} \sqrt{\left|\frac{\partial H}{\partial x}\right|} sgn\left(\frac{\partial H}{\partial x}\right) - k_a(h - d_m)\frac{\partial H}{\partial x} - k_m d_m \frac{\partial H}{\partial x}, & (d_a < h) \end{cases} \qquad (13)$$

4.2.2 Calculation of channel geometry

In RRI model, one dimensional diffusive wave model is used for river channel and the geometry is assumed as rectangle when detail river cross section is not available. The river width and depth are approximated by using the following functions according to the upstream contributing area in square kilometer.

$W = C_w A^{S_w}$

$D = C_D A^{S_D}$

Where,

$W = widthinmeter$

$D = depthinmeter$

$A = Areainsquarekilometer$

$C_w, S_w = widthparameters$

$C_d, S_d = depthparameters$

4.2.3 Interaction between slope and river cells

Water exchange between a slope grid cell and river grid cell is calculated at each time step depending on the relationship among the levels of slope water, river water, levee height and ground. The figure below shows four different conditions and for each condition, different overtopping formulae are applied to calculate the unit length discharge from slope to river (q_{sr}) or from river to slope (q_{rs}), which are then multiplied by the length of the river vector at each grid cell to calculate the total exchange flow rate. (Iwasa, 1982)

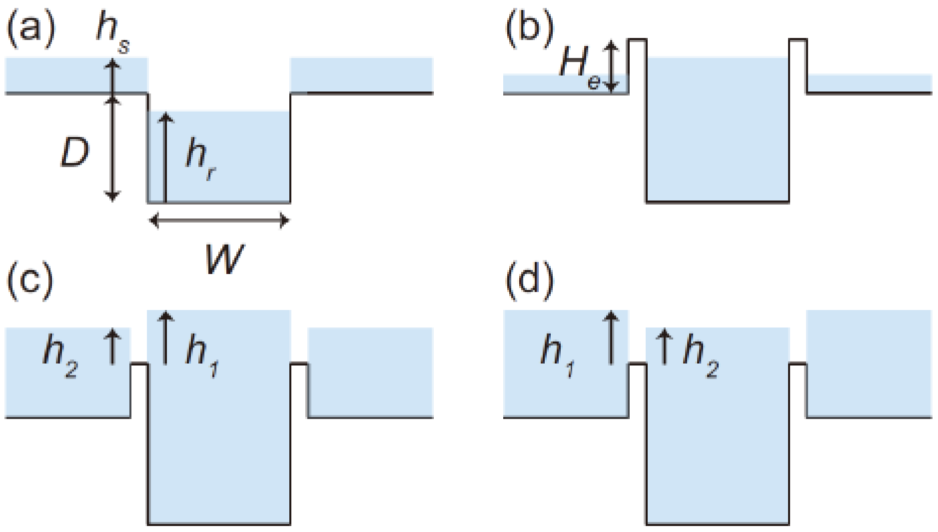

Fig 4.2 River and slope water exchange

(Sayama T. , Rainfall-Runoff-Inundation (RRI) Model, User's Manual)

When water level in the river cell is lower than the ground level, water from the slope cell will flow to the river and the following formula is used for calculation of discharge per unit width.

$$q_{sr} = \mu_1 h_s \sqrt{g h_s}$$

Where,

μ_1= constant coefficient

h_s= water depth on slope cell

4.2.4 Runge-Kutta Method

The Runge-Kutta methods are an important family of iterative methods for the approximation of solution of ordinary differential equations. RRI model use the fifth order Runge-Kutta method with adaptive time step control. This method solve an ordinary differential equation by the general fifth order Runge-Kutta formula and estimate its error by an embedded fourth order formula to control the time step. (Cash. J.R, 1990).The general form of fifth order Runge-Kuttha formula is

$$k_1 = \Delta t f(t, h_1)$$

$$k_2 = \Delta t f(t + a_2 \Delta t, h_1 + b_{21} k_1)$$

$$k_3 = \Delta t f(t + a_3 \Delta t, h_1 + b_{31} k_1 + b_{32} k_2)$$

$$k_4 = \Delta t f(t + a_4 \Delta t, h_1 + b_{41} k_1 + b_{42} k_2 + b_{43} k_3)$$

$$k_5 = \Delta t f(t + a_6 \Delta t, h_1 + b_{61} k_1 + b_{62} k_2 + b_{63} k_3 + b_{64} k_4 + b_{65} k_5)$$

$$h_{t+1} = h_t + c_1 k_1 + c_2 k_2 + c_3 k_3 + c_4 k_4 + c_5 k_5 + c_6 k_6 + O(\Delta t^6)$$

While the embedded forth order formula (Cash. J.R, 1990) is

$$h^*_{t+1} = h_t + c^*_1 k_1 + c^*_2 k_2 + c^*_3 k_3 + c^*_4 k_4 + c^*_5 k_5 + c^*_6 k_6 + O(\Delta t^5)$$

By subtracting $h^*_{t+1} - h_{t+1}$,the error can be estimated by using $k_1 to k_6$ as follows,

$$\delta \equiv h_{i+1} - h^*_t \equiv \sum_{i=1}^{6} (c_i - c^*_i) k_i$$

4.2.5 Infiltration

Infiltration is the process of water entry into a soil from rainfall, snowmelt, or irrigation. Soil water movement is the process of water flow from one point to another within soil. Rate of infiltration is controlled by the rate of soil water movement below the surface and the soil water movement continues after the infiltration event, as infiltrated water is redistributed. The soil properties affecting soil water movement are hydraulic conductivity and water retention characteristic. Hydraulic conductivity is a measure of the ability of the soil to transmit water and depends upon both the properties of soil and the water. Total porosity, pore size distribution, and pore continuity are the important factors affecting hydraulic conductivity. The water retention characteristic of the soil describes the soil's ability to store and release water and is defined as the relationship between the soil water content and the soil suction or metric potential.

4.2.6 Green-Ampt model

The Green-Ampt infiltration model is a simplified physical model and based on the Richard equation. It related the rate of infiltration to measurable soil properties such as the porosity, hydraulic conductivity, and moisture content of a particular soil. The advantages of Green-Ampt infiltration equation to Richard equation are that the analytical solution available for the computation of wetting front location and only two parameters of soil properties are required. The equation for Green-Ampt infiltration model to calculate infiltration losses is as follow.

$$f = k_v \left| 1 + \frac{(\emptyset - \theta_i) S_f}{F} \right|$$

$k_v = verticalsaturatedhydraulicconductivity$

$S_f = suctionattheverticalwettingfront$

$F = cumulativeinfiltrationdepth$

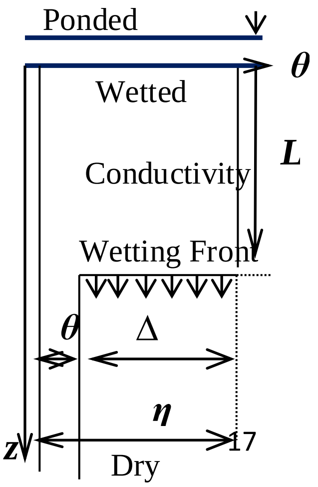

Fig 4.3 Schematic representation of Green and Ampt infiltration model

5. D

Digital Elevation Model Inputs

SRTM DEM of 1 arc Sec has been used in the study. Spatial resolution of DEM is 90 meter, square pixel were used. DEM needs pre processing, including mosaicking, resampling and projection. Projected DEM can be imported in HEC-RAS. DEM can also be processed for retrieval of hydrological & Catchment properties. Catchment and stream were delineated using the DEM as shown in the fig. 5.1.

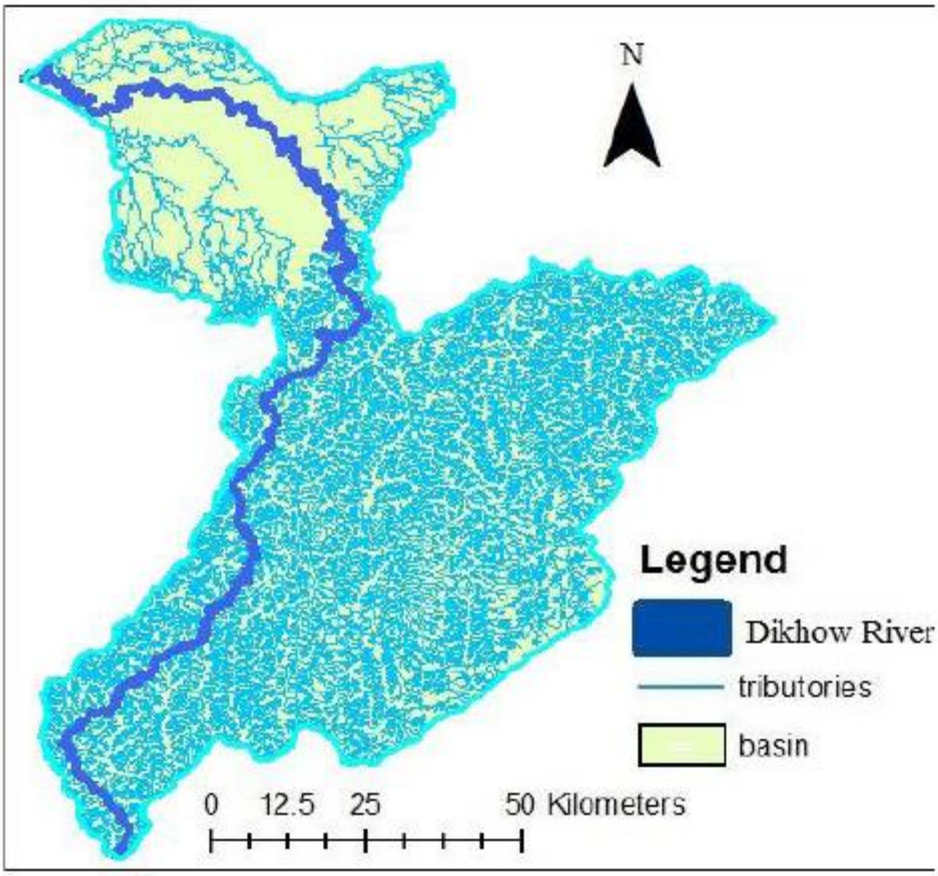

Fig 5.1 **Digitized map of Dikhow river basin and its Tributaries along with its boundaries**

6.0 RESULTS AND DISCUSSION

6.1 Executing RRI Model

The RRI Input files are prepared and 0_rri_1_4_2.exe file is executed for calibration and validation.

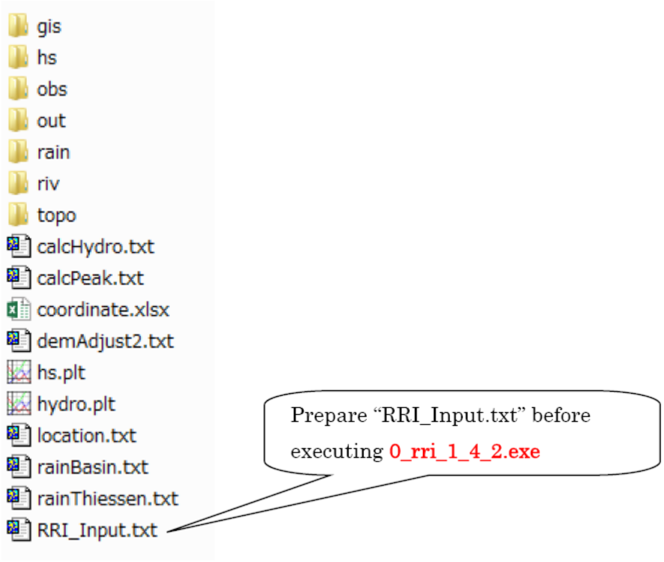

- gis
- hs
- obs
- out
- rain
- riv
- topo
- calcHydro.txt
- calcPeak.txt
- coordinate.xlsx
- demAdjust2.txt
- hs.plt
- hydro.plt
- location.txt
- rainBasin.txt
- rainThiessen.txt
- RRI_Input.txt

Prepare "RRI_Input.txt" before executing **0_rri_1_4_2.exe**

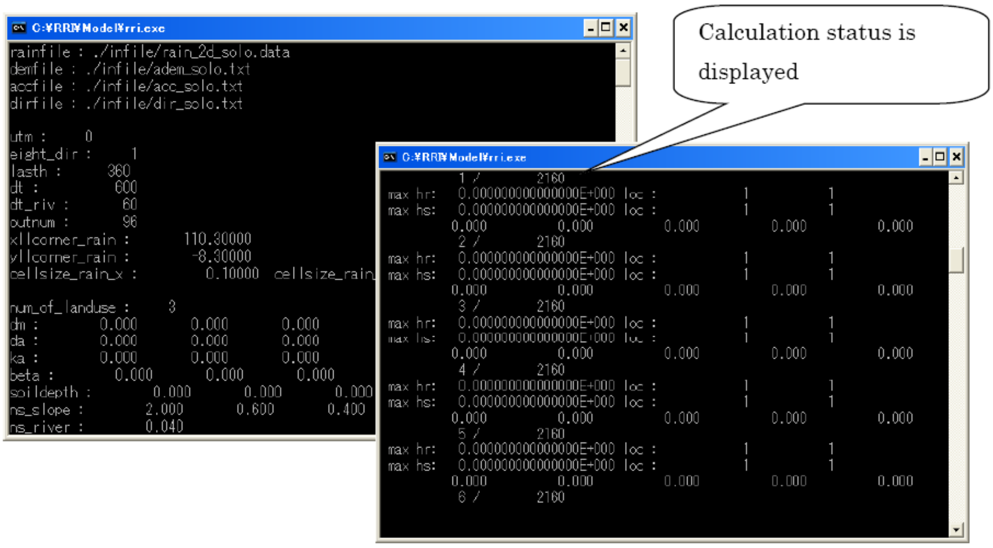

```
rainfile : ./infile/rain_2d_solo.data
demfile : ./infile/adem_solo.txt
accfile : ./infile/acc_solo.txt
dirfile : ./infile/dir_solo.txt

utm :      0
eight_dir :      1
lasth :      360
dt :          600
dt_riv :       60
outnum :       96
xllcorner_rain :       110.30000
yllcorner_rain :        -8.30000
cellsize_rain_x :          0.10000   cellsize_rain

num_of_landuse :     3
dm :         0.000         0.000         0.000
da :         0.000         0.000         0.000
ka :         0.000         0.000         0.000
beta :         0.000         0.000         0.000
soildepth :         0.000         0.000         0.000
ns_slope :        2.000         0.600         0.400
ns_river :        0.040
```

```
          1 /          2160
 max hr:   0.0000000000000000E+000 loc :            1            1
 max hs:   0.0000000000000000E+000 loc :            1            1
         0.000          0.000          0.000          0.000          0.000
          2 /          2160
 max hr:   0.0000000000000000E+000 loc :            1            1
 max hs:   0.0000000000000000E+000 loc :            1            1
         0.000          0.000          0.000          0.000          0.000
          3 /          2160
 max hr:   0.0000000000000000E+000 loc :            1            1
 max hs:   0.0000000000000000E+000 loc :            1            1
         0.000          0.000          0.000          0.000          0.000
          4 /          2160
 max hr:   0.0000000000000000E+000 loc :            1            1
 max hs:   0.0000000000000000E+000 loc :            1            1
         0.000          0.000          0.000          0.000          0.000
          5 /          2160
 max hr:   0.0000000000000000E+000 loc :            1            1
 max hs:   0.0000000000000000E+000 loc :            1            1
         0.000          0.000          0.000          0.000          0.000
          6 /          2160
```

Calculation status is displayed

Fig 6.1 : Inputs required to execute RRI Model

Calibration of RRI Model

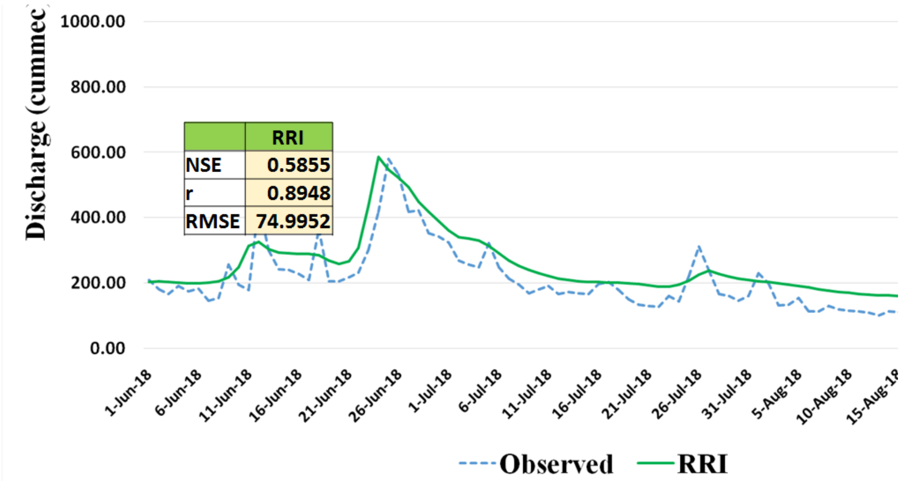

Fig 6.2 RRI Model calibrated from 1 June 18 to 15 August 18

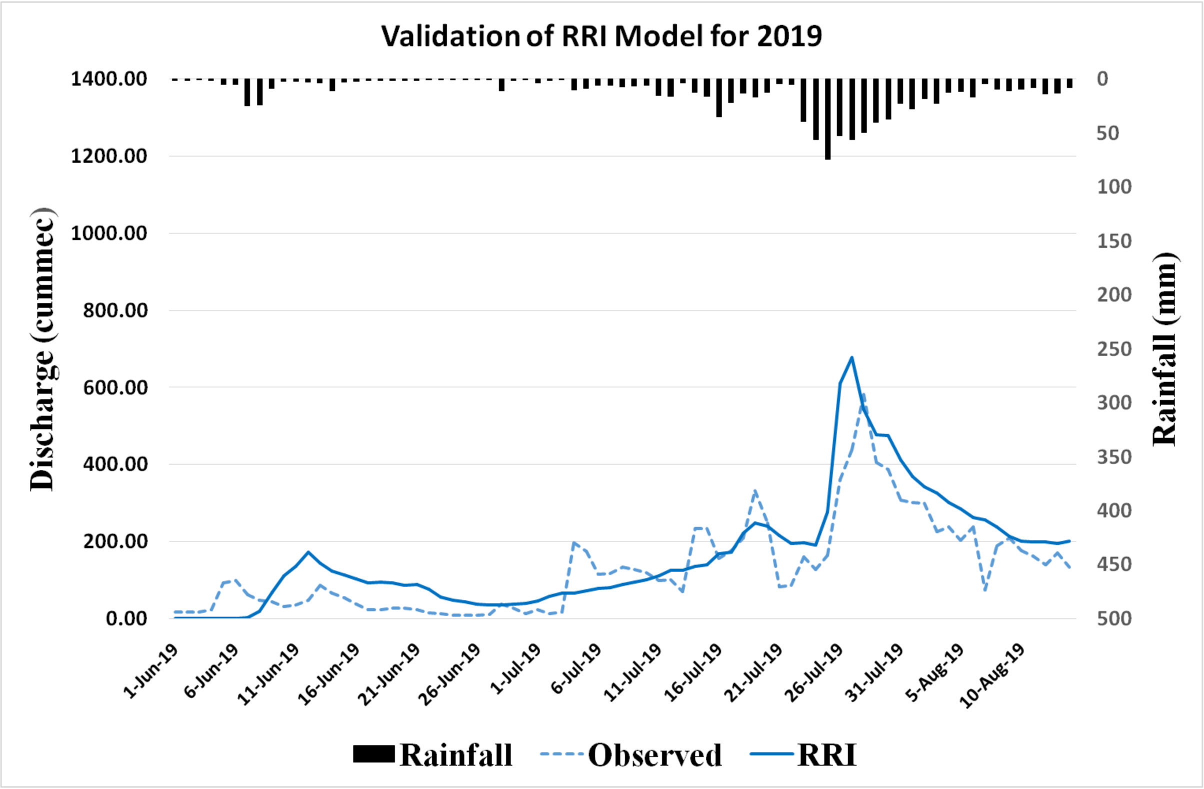

The validated RRI model showed an NSE of 0.5855, r = 0.8948 and RMSE = 74.9952

Inundation Extent predicted by RRI model

The inundation extent predicted by the RRI model is shown in figure. The top portion of the basin near the outlet is completely inundated as shown in the figure.

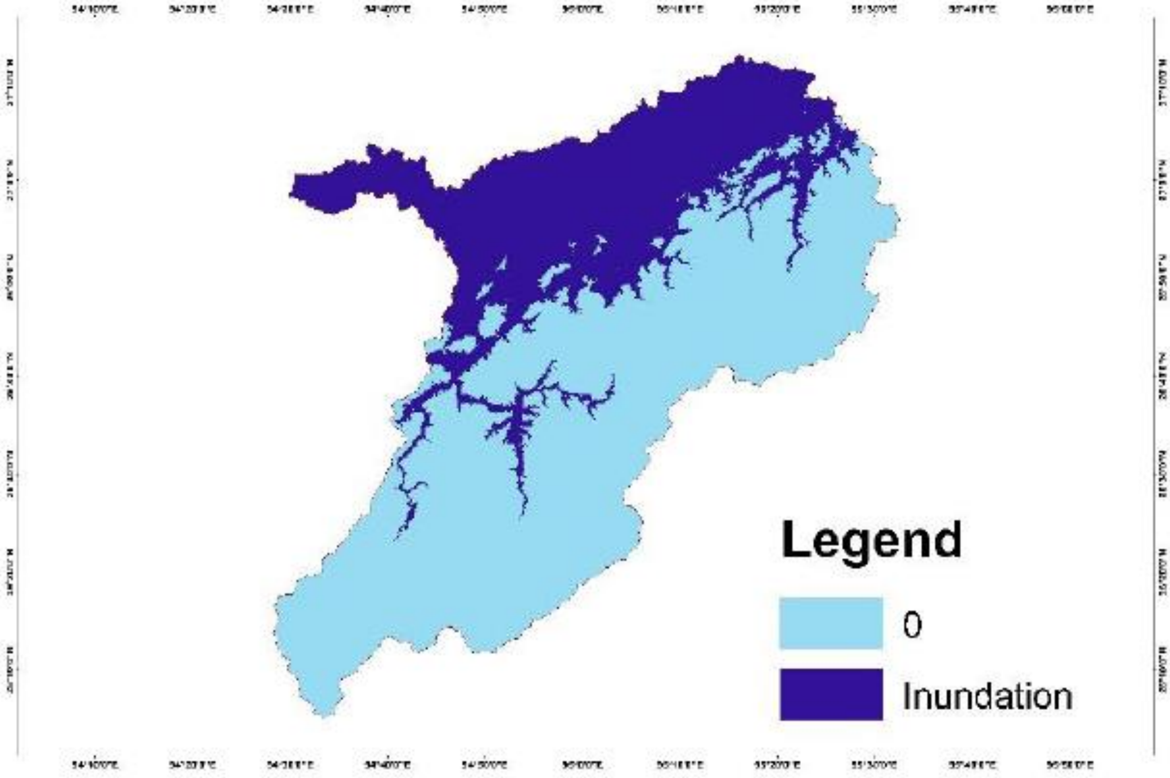

Fig6.3 Inundation Extent Predicted by RRI Model

The depth vs inundation extent is shown in Table.1 A total of 7m depth is observed for the Dikohw River Basin. A total of 1143.109 Km^2 of Area is observed to be under inundation. A maximum inundation of 359.211 km^2 is observed for 1m depth.

Table. 1 Inundation depth vs extent of Dikhow watershed

Inundation Depth (m)	Inundation Extent (km^2)
1	359.211
2	248.762
3	158.968
4	140.662
5	120.727
6	73.321
7	41.458
Sum	**1143.109**

7.0 CONCLUSION AND DISCUSSIONS

- A total of 1,143 km^2 of area was found to be maximum inundated.
- Comparison of Predicted discharge with RRI model predictions showed that RRI model predictions followed the trends of observed discharge values, however under predicted the peaks

Floods can cause a tremendous amount of damage, especially in the highly regulated river sectors overlaid with highly urbanized areas along the floodplain. For this reason, the multiple viewpoints, methods, assumptions, and future possibilities adapted to new trends (social, economic, natural) and determined by different factors, play an important role in the flood hazard management and establishing flood-vulnerable areas. Even in a highly regulated river system, flood hazards exist; properties and lives are in danger. A flash flood, dense precipitation, or an error in the discharge flow at the gates of the reservoirs can turn into a catastrophic flood event. For this reason, a good preparation regarding this topic is always welcomed. As remote sensing (RS) techniques continue to improve and the availability of data increases, more RS data will be integrated and used in flood modelling. A better horizontal and vertical accuracy is required on flat terrain (such as wide floodplains) and the integration of vegetation and building heights (urban areas) offer the perfect support for flood hydraulic simulations and accurate water flow propagation. Manually integration of building heights in the case of data unavailability of surface model can be a better solution. The 2D hydraulic modelling multi-scenario results can be exported into a set of flood hazard parameters such as flood depth, flood extent, flood velocity, or water surface elevation; and can answer real questions regarding the flood hazard threat at local level. Developing stream flow scenarios on a small-scale level is a very important aspect for any flood mitigation effort, especially in the urban areas located along main rivers, because large-scale analysis (river basin analysis) understates flood risk perception.

7.0 REFERENCES

Arun, G., Sharma,S. K., Tirkey,G., and Lohani,A. K. (2020). “Integrated Flood Assessment Studies Using Real Time Satellite Precipitation Data and Flood Inundation Mapping in Assam - A Novel Approach.” National Conference on Emerging Trends in Civil Engineering, pp: 0-19.

Bhattacharya, B., Conway, C., Solomatine, D., Masih, I., Craven, J., Mazumder, L. C., Mazzoleni, M., Ugay, R., van Andel, S. J., & Shrestha, S. (2018). Hydrological and Erosion Modelling of the Brahmaputra Basin Using Global Datasets. 3, 245–237.

Bhattacharya, B., Mazzoleni, M., &Ugay, R. (2019). Flood inundation mapping of the sparsely gauged large-scale Brahmaputra basin using remote sensing products. Remote Sensing, 11(5), 1–23.

Brunner G. W (2018). HEC-RAS, River Analysis System Hydraulic Reference Manual, US Army Corps of Engineers, Hydrologic Engineering Center(HEC), CA 95616-4687, CPD-69

Brunner G. W (2018). HEC-RAS, River Analysis System Supplemental User’s Manual Version 5.0.4, US Army Corps of Engineers, Hydrologic Engineering Center(HEC), CA 95616-4687, CPD-68d.

Brunner G. W. et al (2018). HEC-RAS, River Analysis System Application Guide, Supplemental User’s Manual Version 5.0.4, US Army Corps of Engineers, Hydrologic Engineering Center(HEC), CA 95616-4687, CPD-70.

Central Water Commission (CWC) & National Remote Sensing Centre (NRSC). (2014). Brahmaputra Basin Version 2.0. 127. http://www.india-wris.nrsc.gov.in/wris.html

Dadhwal, V.K.,Kumar, R., Sharma, J.R.,Tembhurney, W.M.,Bera, A.K.,Paithankar, Y., Paliwal, R., Kalsi, A.P.,Chauhan, N., Bhati, G., Shirsath, P.B.,Bankar, N., V. S. and H. S. (2012). *River basin atlas of India.*

Elfeki, A., Al-Shabani, A., Bahrawi, J., &Alzahrani, S. (2018). Quick Urban Flood Risk Assessment in Arid Environment Using HECRAS and Dam Break Theory: Case Study of Daghbag Dam in Jeddah, Saudi Arabia. 2010, 1917–1919. https://doi.org/10.1007/978-3-319-70548-4_553

Farooq, M., Shafique, M., &Khattak, M. S. (2019). Flood hazard assessment and mapping of River Swat using HEC-RAS 2D model and high-resolution 12-m TanDEM-X DEM (WorldDEM). Natural Hazards, 97(2), 477–492.

Goodell, C., Warren, C. (2006). Flood Inundation Mapping using HEC-RAS. Obras y Proyectos, 18–23.

Horritt, M.S., Bates P.D., (2002).Evaluation of 1D and 2D numerical models for predicting river floodflood inundation. Journal of Hydrology, 268 (2002) 87–99

Jain, S. K., Mani, P., Jain, S. K., Prakash, P., Singh, V. P., Tullos, D., Kumar, S., Agarwal, S. P., &Dimri, A. P. (2018). A Brief review of flood forecasting techniques and their applications. International Journal of River Basin Management, 16(3), 329–344.

Lea, D., Yeonsu, K., &Hyunuk, A. (2019). Case study of HEC-RAS 1D-2D coupling simulation: 2002 Baeksan flood event in Korea. Water (Switzerland), 11(10), 1–14.

Mihu-Pintilie, A., Cîmpianu, C. I., Stoleriu, C. C., Pérez, M. N., &Paveluc, L. E. (2019). Using high-density LiDAR data and 2D streamflow hydraulic modeling to improve urban flood hazard maps: A HEC-RAS multi-scenario approach. Water (Switzerland), 11(9).

Patel, D. P., Ramirez, J. A., Srivastava, P. K., Bray, M., & Han, D. (2017). Assessment of flood inundation mapping of Surat city by coupled 1D/2D hydrodynamic modeling: a case application of the new HEC-RAS 5. Natural Hazards, 89(1), 93–130.

Rangari, V. A., Umamahesh, N. V., & Bhatt, C. M. (2019). Assessment of inundation risk in urban floods using HEC RAS 2D. Modeling Earth Systems and Environment, 5(4), 1839–1851.

Salunkhe, S. S., Rao, S. S., Prabu, I., Raghu Venkataraman, V., Krishna Murthy, Y. V. N., Sadolikar, C., & Deshpande, S. (2018). Flood Inundation Hazard Modelling Using CCHE2D Hydrodynamic Model and Geospatial Data for Embankment Breaching Scenario of Brahmaputra River in Assam. Journal of the Indian Society of Remote Sensing, 46(6), 915–925.

Sarma J. N. and Acharjee S. (2018). A Study on Variation in Channel Width and Braiding Intensity of the Brahmaputra River in Assam, India. MDPI, Geosciences 2018, 8, 343. PP. 1-19

Sharma, S. K. (2011). Status report on flood inundation and flood hazard mapping with special reference to Brahmaputra in North East India. Annual Report. 2011, pp. 1-57.

Singh, V.P., Sharma, N. and Ojha C.S.P. “The Brahmaputra Basin Water Resources” (eds.) (2004): ISBN 1-4020-1737-5 1-610p

Timbadiya, P. V., Patel, P. L., &Porey, P. D. (2011). Calibration of HEC-RAS Model on Prediction of Flood for Lower Tapi River, India. Journal of Water Resource and Protection, 03(11), 805–811.

Vojtek, M., Petroselli, A., Vojteková, J., &Asgharinia, S. (2019). Flood inundation mapping in small and ungauged basins: Sensitivity analysis using the EBA4SUB and HEC-RAS modeling approach. *Hydrology Research*, *50*(4), 1002–1019.

Yalcin, E. (2020). Assessing the impact of topography and land cover data resolutions on two-dimensional HEC-RAS hydrodynamic model simulations for urban flood hazard analysis. *Natural Hazards*, *101*(3), 995–1017.

Zope, P. E., Eldho, T. I., &Jothiprakash, V. (2017). Hydrological impacts of land use–land cover change and detention basins on urban flood hazard: a case study of Poisar River basin, Mumbai, India. *Natural Hazards*, *87*(3), 1267–1283.